

Joint Helmholtz-Rosatom School and
ITEP Winter School of Physics “Extreme State of Matter”

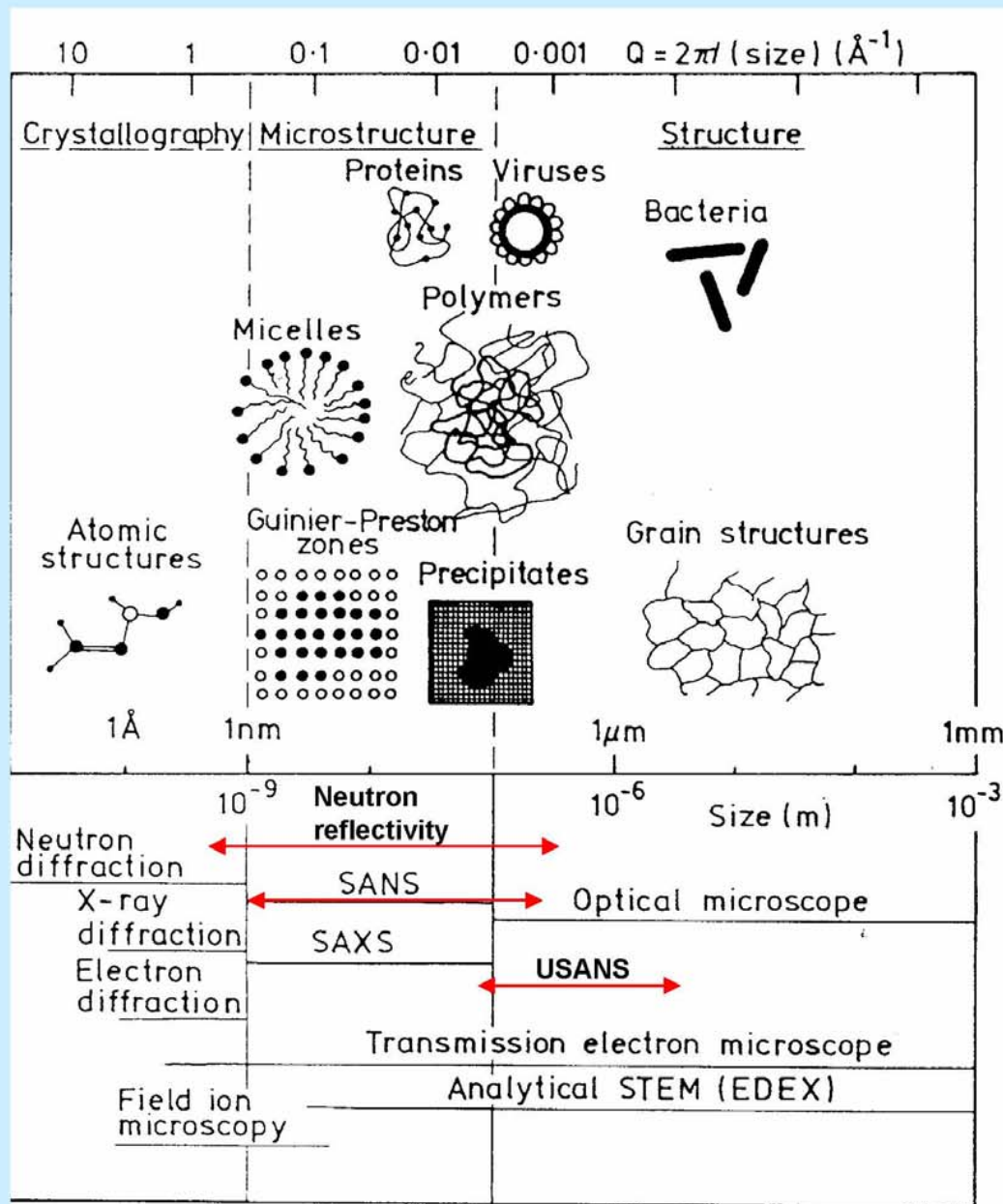
NEUTRON STUDIES OF CONDENSED MATTER

D. Lvov, F. Dzheparov

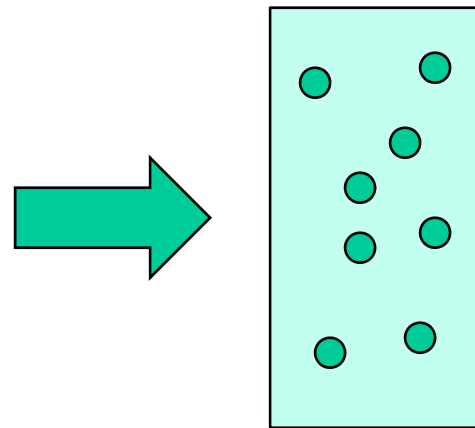
*Institute for Theoretical and
Experimental Physics, Russia,
Moscow*



Techniques for the Measurement of Microstructure



Single scattering

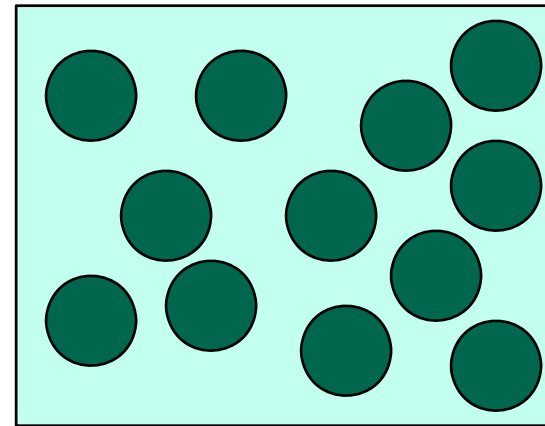


$$l \ll l_c$$

Neutron free path

$$l_c = \frac{1}{c\sigma_t}$$

Multiple scattering



$$l \gg l_c$$

Born parameter

$$\nu = \frac{U_0}{2E} ka = \frac{U_0 a}{\hbar v}$$

Diffraction: $\nu \ll 1$, $\sigma_t = 2\pi a^2 \nu^2$

Refraction: $\nu \gg 1$, $\sigma_t = 2\pi a^2$

Single small angle neutron scattering. Theory.

General Results for a Two Phase System

$$\frac{d\Sigma}{d\Omega}(\vec{q}) = \frac{1}{V} (\rho_1 - \rho_2)^2 \left| \int_{V_1} e^{i\vec{q}\cdot\vec{r}} d\vec{r}_1 \right|^2$$

'Particles' (i.e. discrete inhomogeneities)

Non-particulate systems

$$I(q) = \frac{N}{V} (\rho_1 - \rho_2)^2 \langle |F(q)|^2 \rangle S(q)$$

contrast

single particle shape

$$\left| \int_{V_p} e^{i\vec{q}\cdot\vec{r}} d\vec{r} \right|^2$$

interparticle correlations

$$I(q) \propto (\rho_1 - \rho_2)^2 \int_V \gamma(\vec{r}) e^{-i\vec{q}\cdot\vec{r}} d\vec{r}$$

correlation function

Multiple SANS. Moliere's formula.

Basic assumption: scatterers are uncorrelated.

For small angle scattering

scattering vector

$$\mathbf{q} \perp \mathbf{k}_0$$

wave vector of incident neutron

Let us introduce a vector

$$\boldsymbol{\theta} = \frac{\mathbf{k} - \mathbf{k}_0}{|\mathbf{k}_0|} \perp \mathbf{k}_0$$

The scattering problem is equivalent to diffusion in the plane of $\boldsymbol{\theta}$

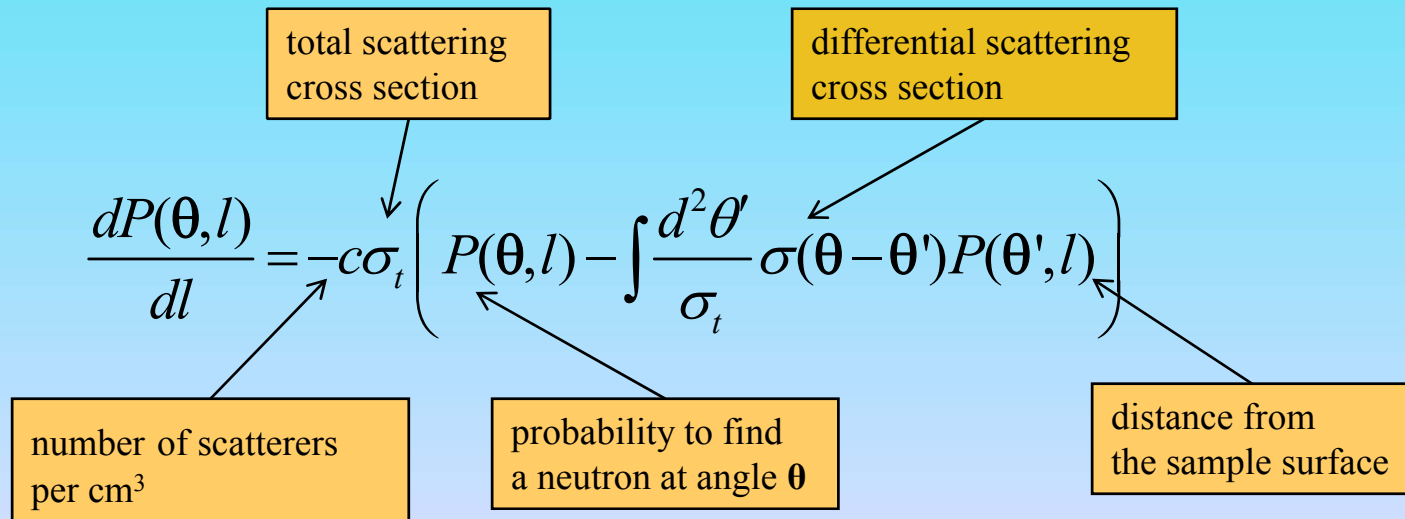
In this case the MSANS theory remains analytical to the end!

Two equivalent approaches

Moliere – considering
successive collisions

Bethe – solution of
transport equation

The standard transport equation



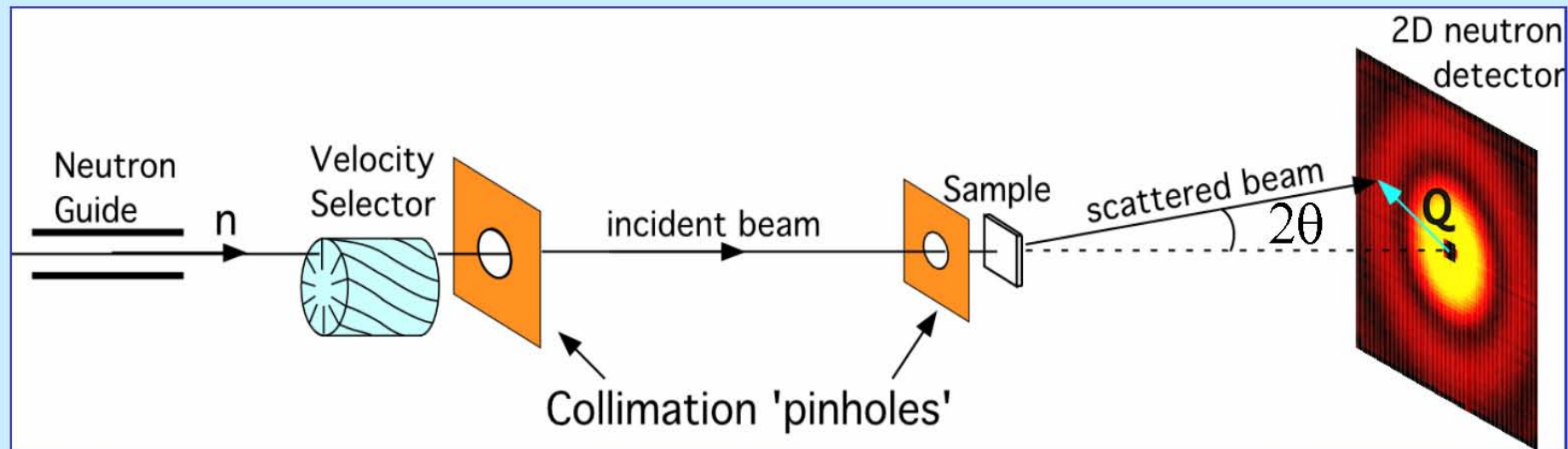
Equation is translationally invariant.

It can be solved by a Fourier transform.

$$P(\theta, l) = \int d^2u \exp(i\mathbf{u}\theta) \exp(-cl[\sigma(0) - \sigma(\mathbf{u})])$$

$$\sigma(\mathbf{u}) = \frac{1}{(2\pi)^2} \int d^2\theta \exp(-i\mathbf{u}\theta) \sigma(\theta)$$

SANS Instrument Schematic



Small-Angle Neutron Scattering (SANS) probes structure on a scale d , where

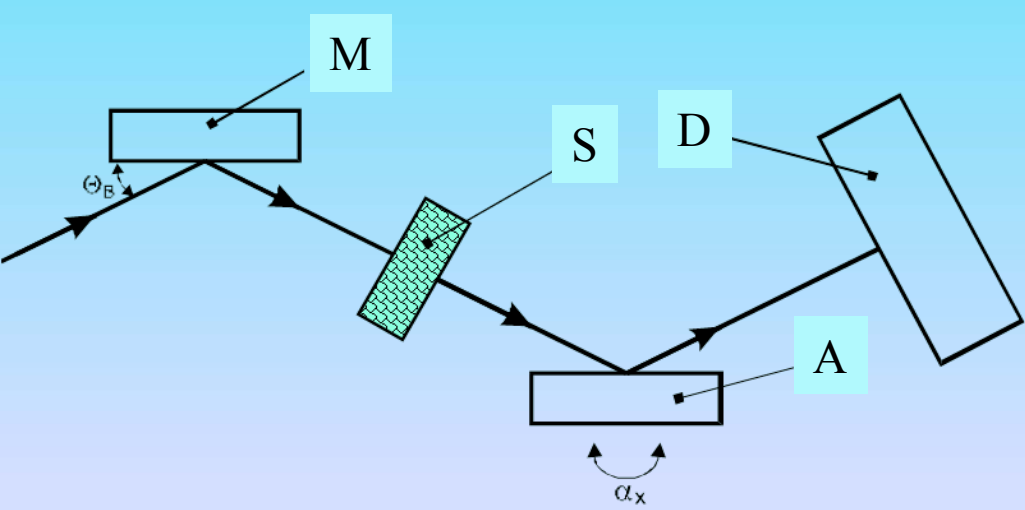
$$d \approx \frac{\lambda}{2\theta} \text{ (wavelength)}$$
$$d \approx \frac{\lambda}{2\theta} \text{ (scattering angle)}$$

$0.5 \text{ nm} < \lambda < 2 \text{ nm}$ (cold neutrons)

$0.1^\circ < \theta < 10^\circ$ (small angles)

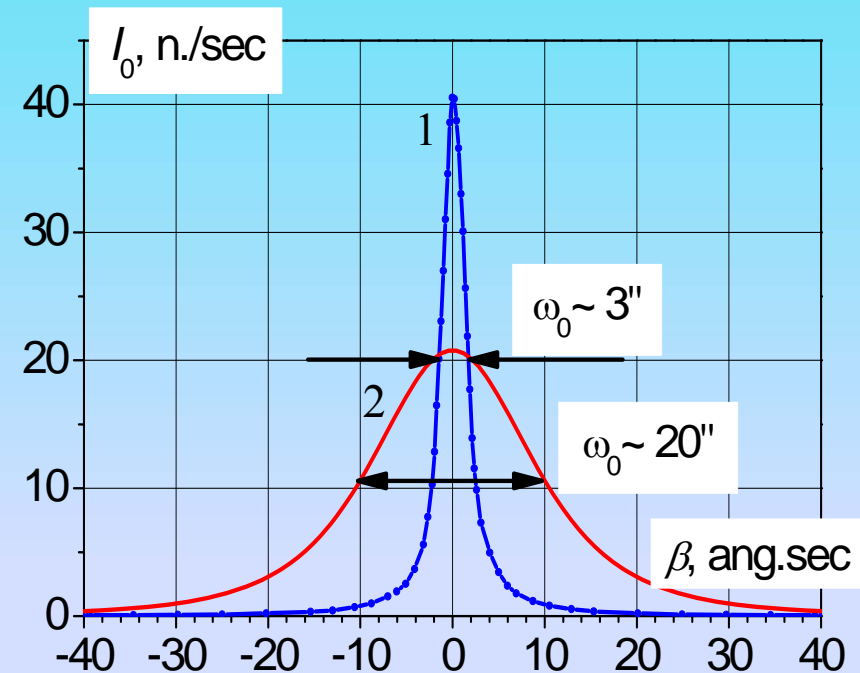
$1 \text{ nm} < d < 300 \text{ nm}$

Double crystal diffractometer schematic.



M and **A** are monochromator and analyzer crystals,
S is a sample and **D** is a detector.

α_x is an angle of rotation, θ_B is the Bragg angle.
Intensity of neutrons on the detector **D**
is measured as a function of rotational
angle α_x of the analyzer.



- 1) Instrumental line of DCD $I_{ins}(\beta)$ at $\lambda = 1,75 \text{ \AA}$
- 2) becomes SANS curve when a sample is placed between crystals

The experimentally observed dependence of the beam intensity on the analyzing crystal rotation angle β

$$I(\beta) = \int_{-\infty}^{\infty} dk \tilde{P}(\beta - \alpha) I_{ins}(\alpha) = \frac{1}{\pi} \int_0^{\infty} dx \cos(\beta x) \tilde{P}(x) I_{ins}(x)$$

where $I_{ins}(x)$ is a Fourier transform of instrumental line $I_{ins}(\alpha)$



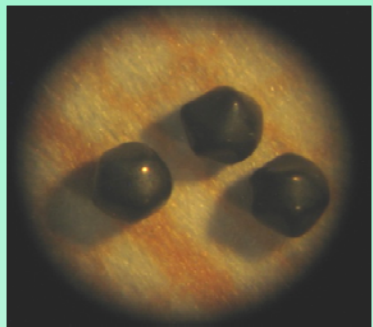
$$\tilde{P}(\alpha) = F_t \delta(\alpha) + F_s(\alpha)$$

instrumental line

$$I(\beta) = F_t I_{ins}(\beta) + I_s(\beta)$$

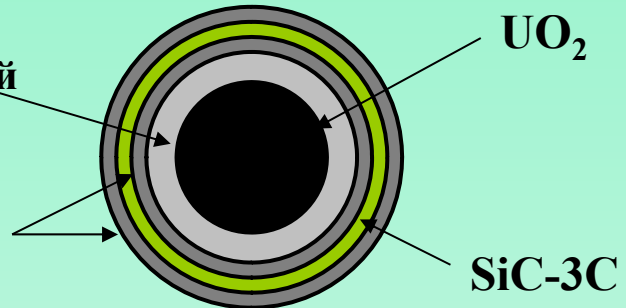
Нейтронно-синхротронная диагностика микротвэлов

Строение микротвэлов



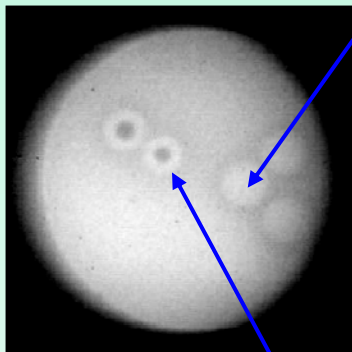
Пироуглерод низкой
плотности

Пироуглерод
высокой плотности

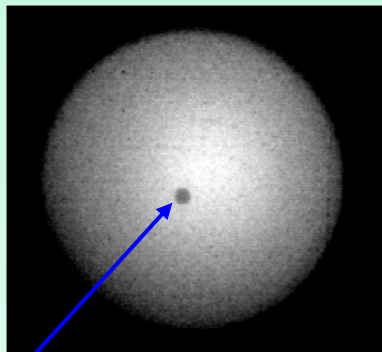


Нейтронная радиография микротвэлов

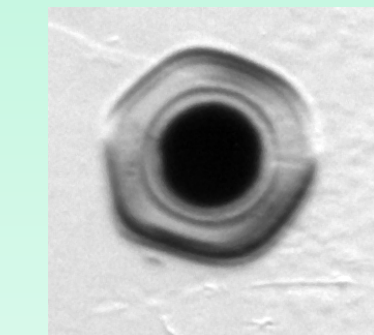
Алмазный фильтр, экспозиция 30 мин
Необогащенные микротвэлы



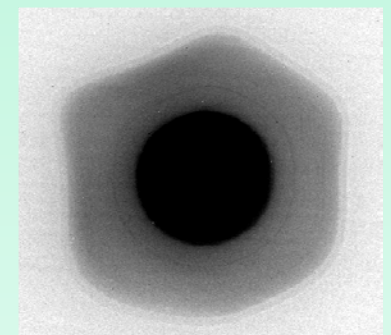
Обогащенные микротвэлы



Рентгеновская радиография на КИСИ (Медиана)



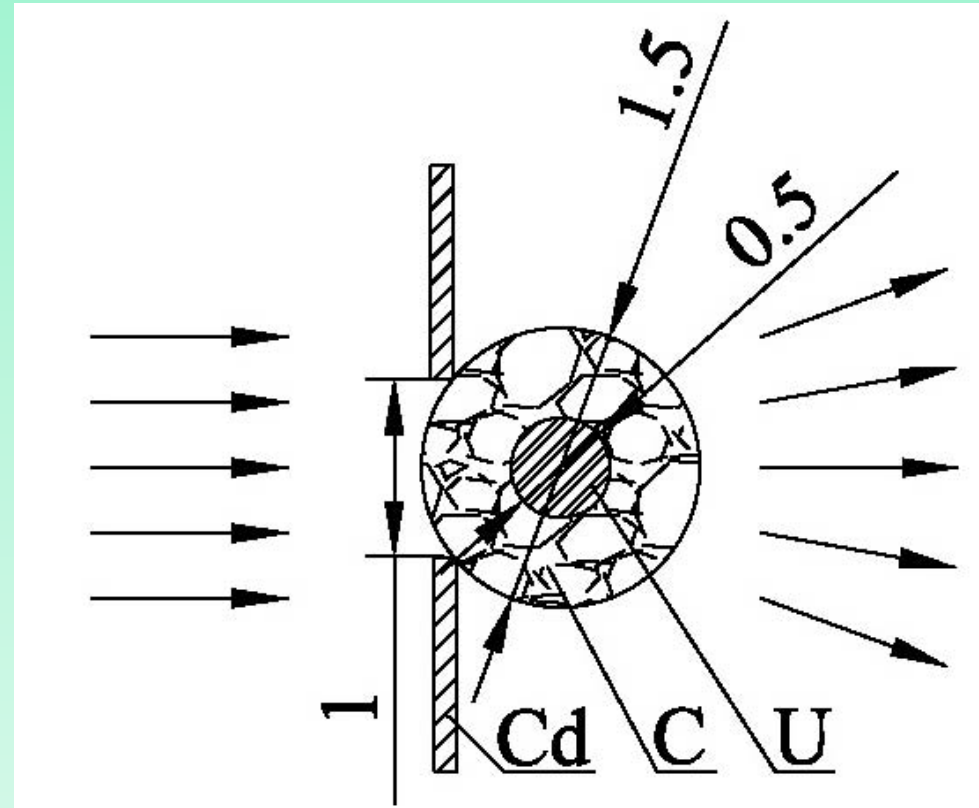
Детектор Imaging Plate,
разрешение 25 мкм



Сцинтиляционный детектор,
разрешение ~ 2 мкм

Small Angle Study of Fuel Particle Coatings

Schematic of CFP sample mounting into a cadmium plate. The hole diameter in the cadmium sheet is ~1 mm, the uranium core diameter is ~0.5 mm, and the diameter of the entire CFP is ~1.5 mm.



The ratio of the numbers of transmitted and incident neutrons

$$\alpha = \exp(-l_U n(0.36\sigma_1 + 0.64\sigma_2)) = 0,67$$

enriched by ^{235}U
to 36%

Theoretical analysis

The experimentally observed dependence of the beam intensity on the analyzing crystal rotation angle β

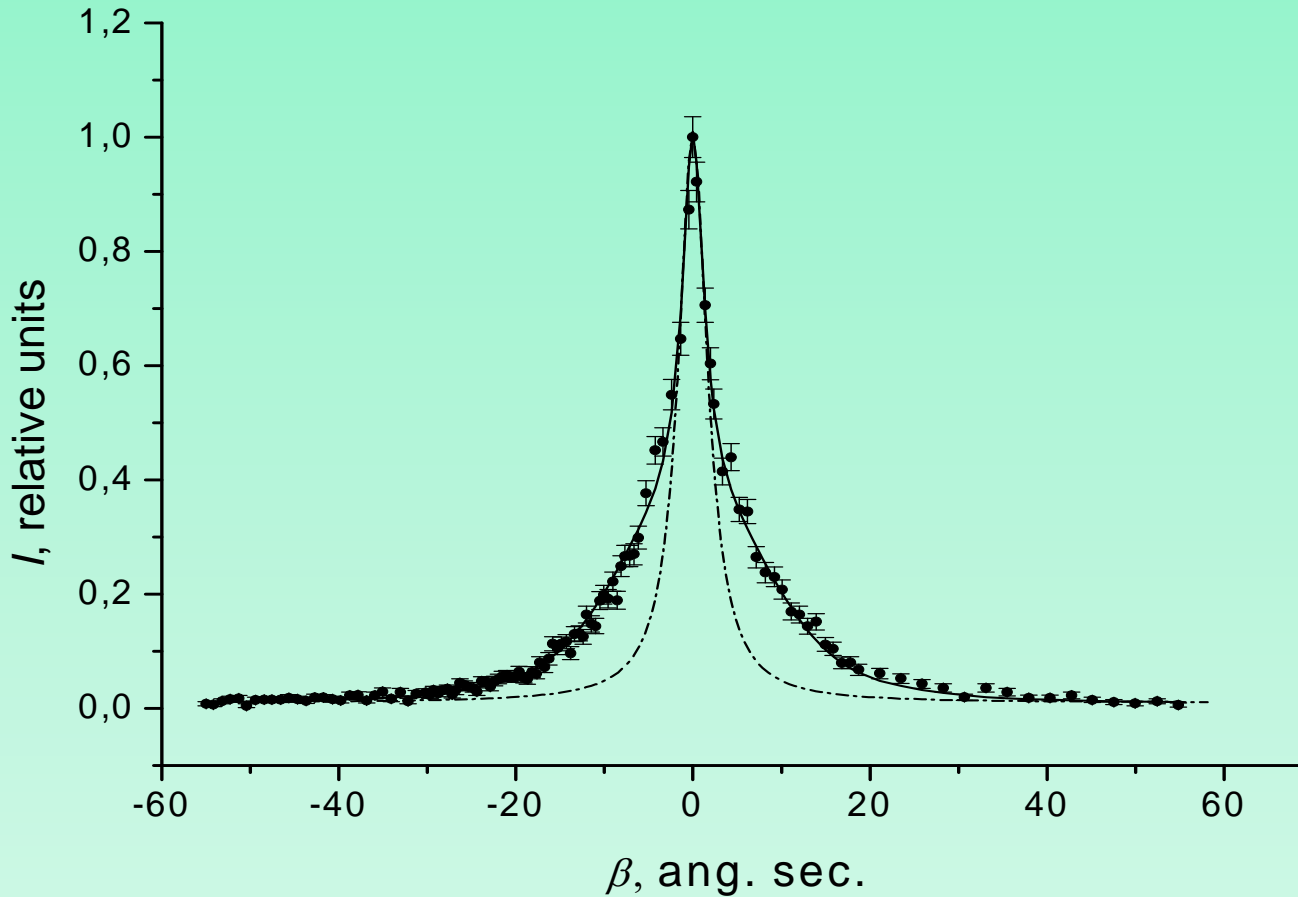
$$I^{\text{exp}}(\beta) = \frac{S_1}{\pi} \int_0^\infty dy \cdot \cos(\beta y) \exp(-\omega_0 y / 2) \cdot \exp\left[-\frac{L_1}{l}(1 - \sigma_y / \sigma_0)\right] + \\ + \underbrace{\alpha \frac{S_2}{\pi} \int_0^\infty dy \cdot \cos(\beta y) \exp(-\omega_0 y / 2) \cdot \exp\left[-\frac{L_2}{l}(1 - \sigma_y / \sigma_0)\right]}_{\text{neutrons passing through the uranium core}}$$

The differential scattering cross section on an inhomogeneity of radius R

$$\sigma(\theta) = 4(kR)^2 \sigma_0 \frac{(\sin kR\theta - kR\theta \cos kR\theta)^2}{(kR\theta)^6}$$

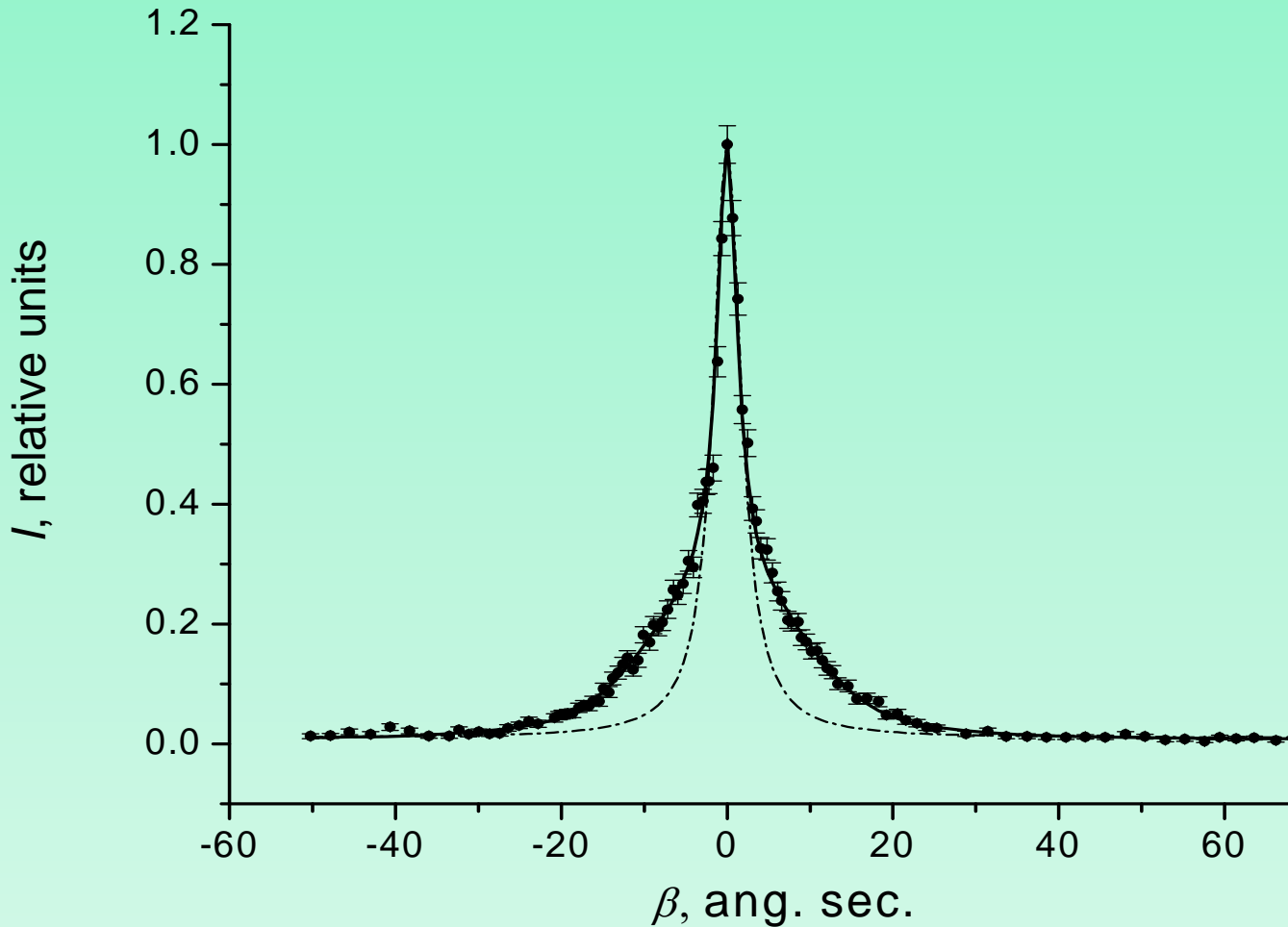
The parameters R and specific volume η (the ratio of the scatterer and sample volumes) were varied to achieve good fit between experimental and calculated curves

USANS curves



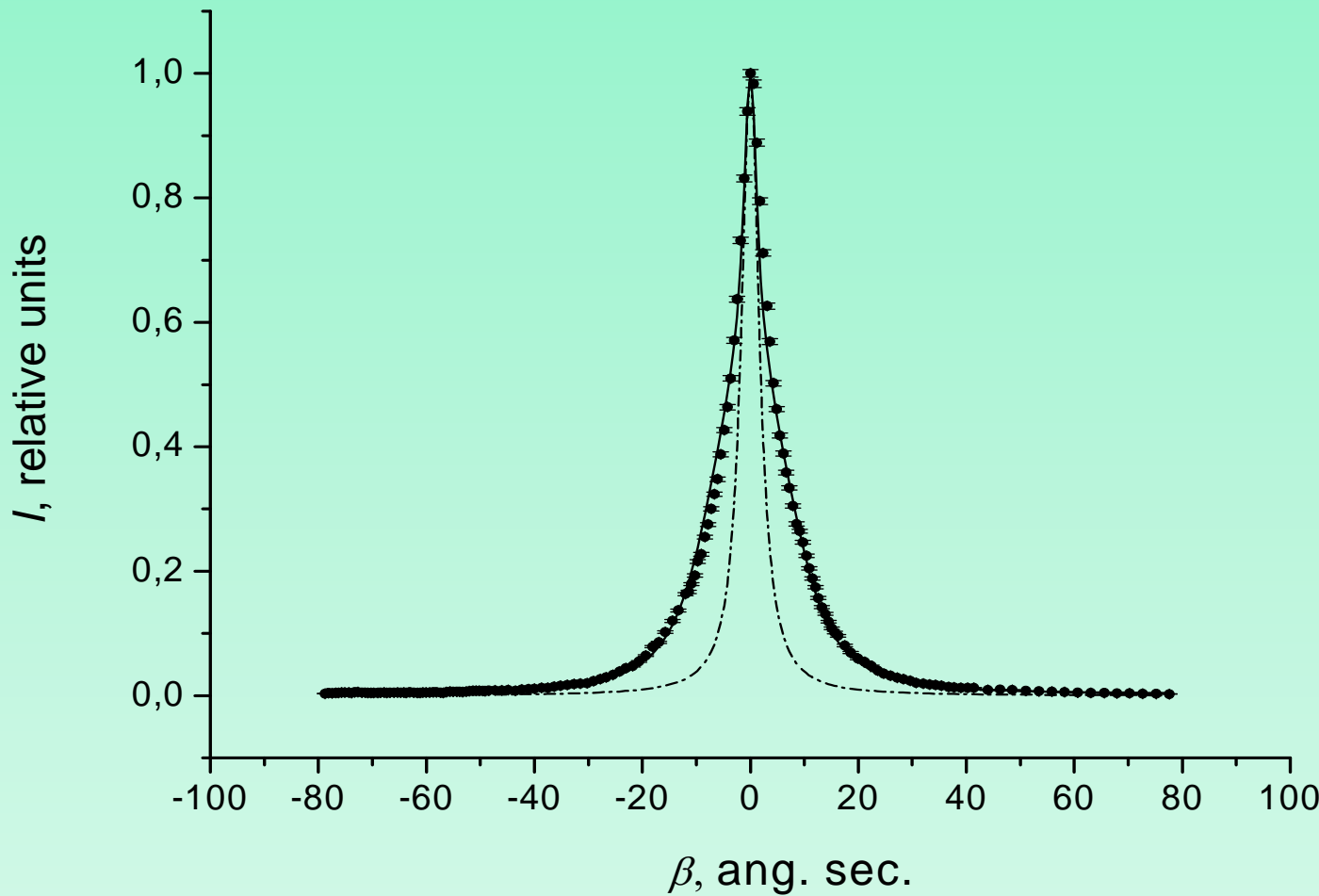
SANS angular distributions for core 1-1, measured using the doublecrystal diffractometer (dots), and their Moliere approximation (solid curve). Dashdotted curve is the instrumental line of the diffractometer. Curves are normalized to unity at the maximum.

USANS curves



SANS angular distributions for core 1-5, measured using the doublecrystal diffractometer (dots), and their Moliere approximation (solid curve). Dashdotted curve is the instrumental line of the diffractometer

USANS curves



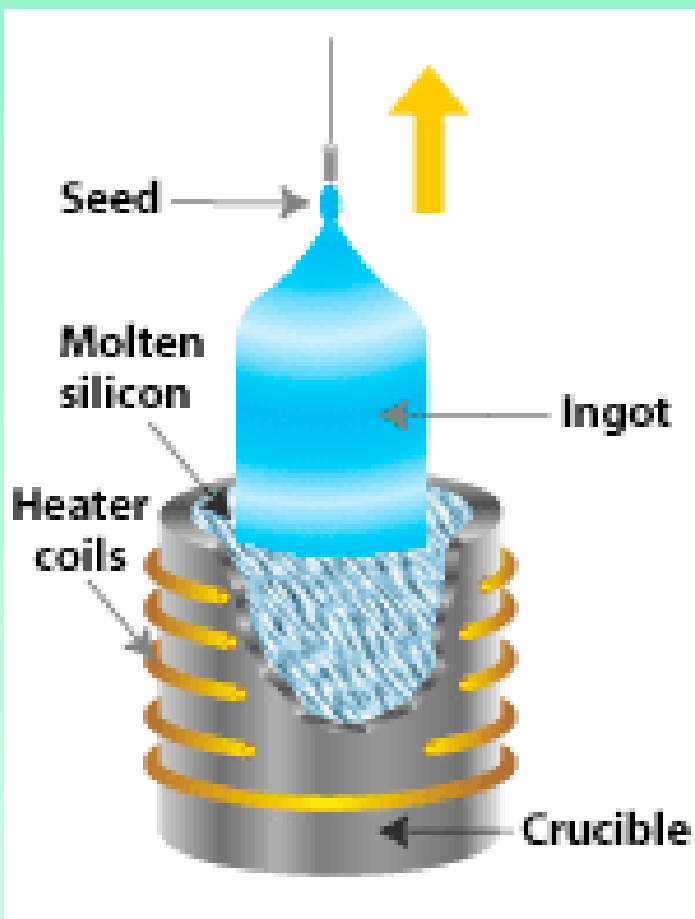
SANS angular distribution for a set of 32 cores, measured using the doublecrystal diffractometer (dots), and its Moliere approximation (solid curve). Dashdotted curve is the instrumental line of the diffractometer.

Results

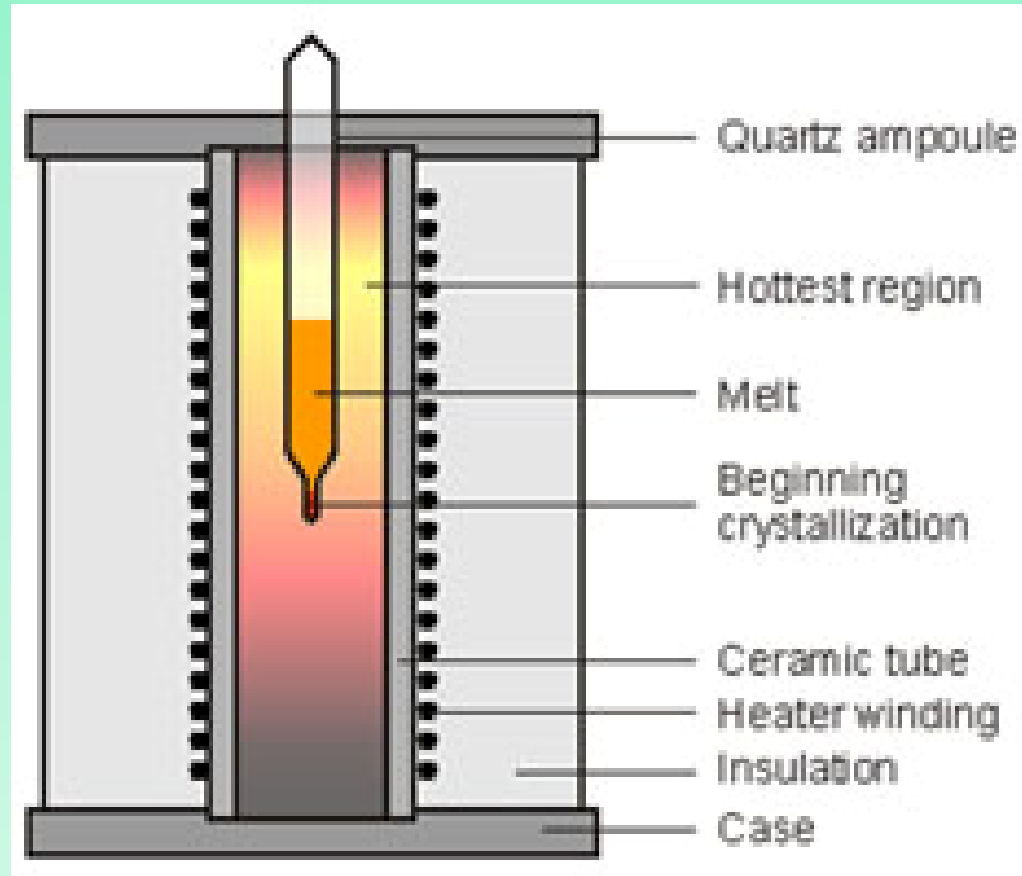
Sample	Pore size $R, \mu\text{m}$	Specific volume η
Core 1-1	1.02(5)	0.048(2)
Core 1-2	1.14(4)	0.034(2)
Core 1-3	0.86(4)	0.043(3)
Core 1-4	1.45(5)	0.063(3)
Core 1-5	0.88(6)	0.042(3)
Core 1-6	1.10(6)	0.023(4)
Core 1-7	1.36(5)	0.062(3)
32 cores	1.28(1)	0.052(1)

- N.O. Elyutin, D.V. Lvov, E.V. Rakshun, A.N. Tyulyusov. *Journal of Surface Investigation. Xray, Synchrotron and Neutron Techniques*, 2010, Vol. 4, No. 6, pp. 908–912

Single crystals growing techniques

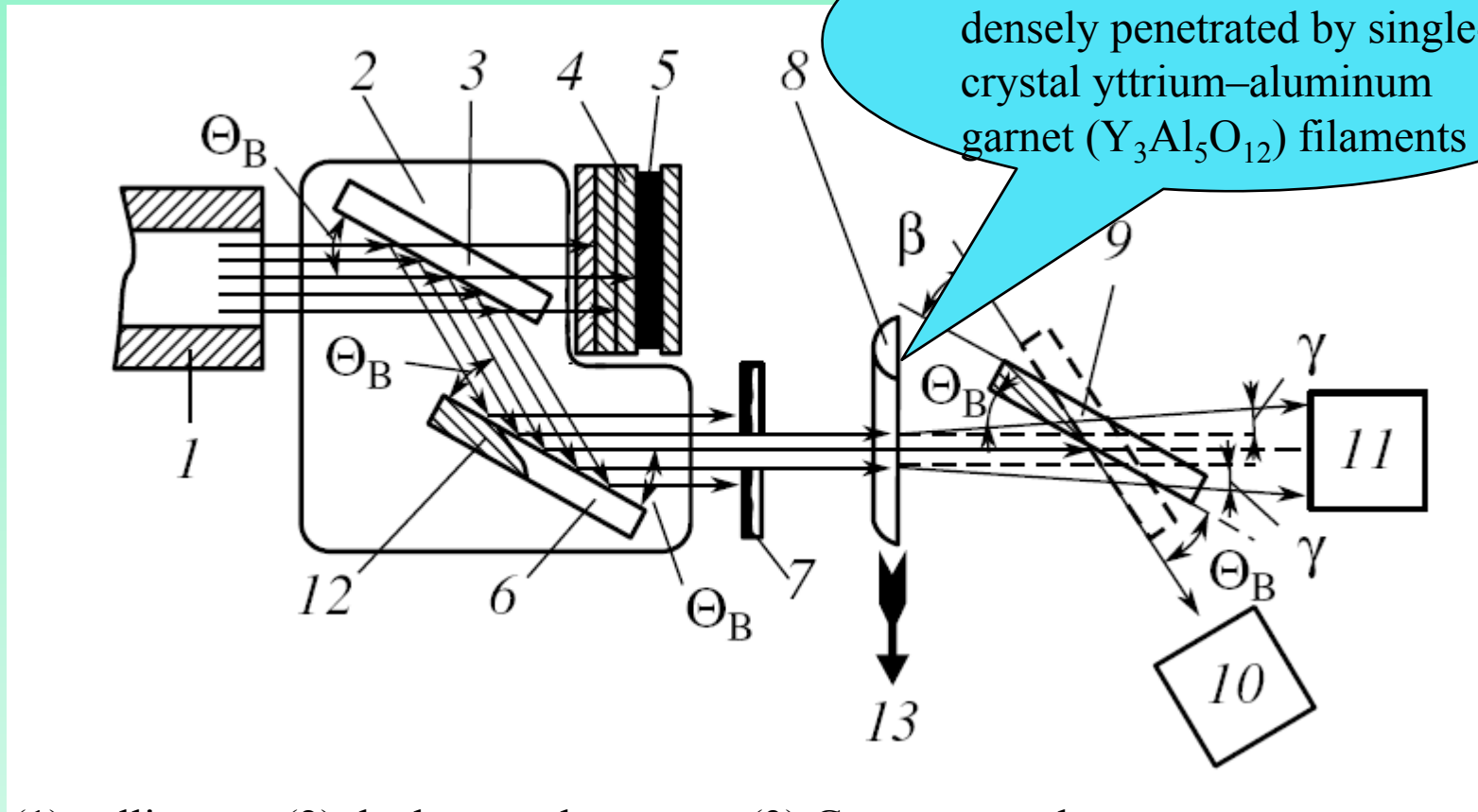


Czochralski apparatus



Bridgman-Stockbarger furnace

Scheme of DCD experiment



- (1) collimator, (2) dual monochromator, (3) Ge premonochromator, (4) protection of monitoring chamber against direct neutron and gamma-ray beams, (5) monitoring chamber, (6) basic Ge monochromator, (7) slotted mask, (8) test sample, (9) Ge crystal analyzer, (10) basic detector to record doubly reflected neutrons, (11) additional detector to record neutrons passing through crystal analyzer, (12) crystallographic planes, and (13) sample motion direction.

Классический метод Уоррена

Скорость счёта N на детекторе Δ_P

$$N = T_0 \cdot T_S \cdot I_{ins} (\beta = 0)$$

немалоугловое рассеяние
МУР

$$N' = T_0 \cdot I_{ins} (\beta = 0)$$

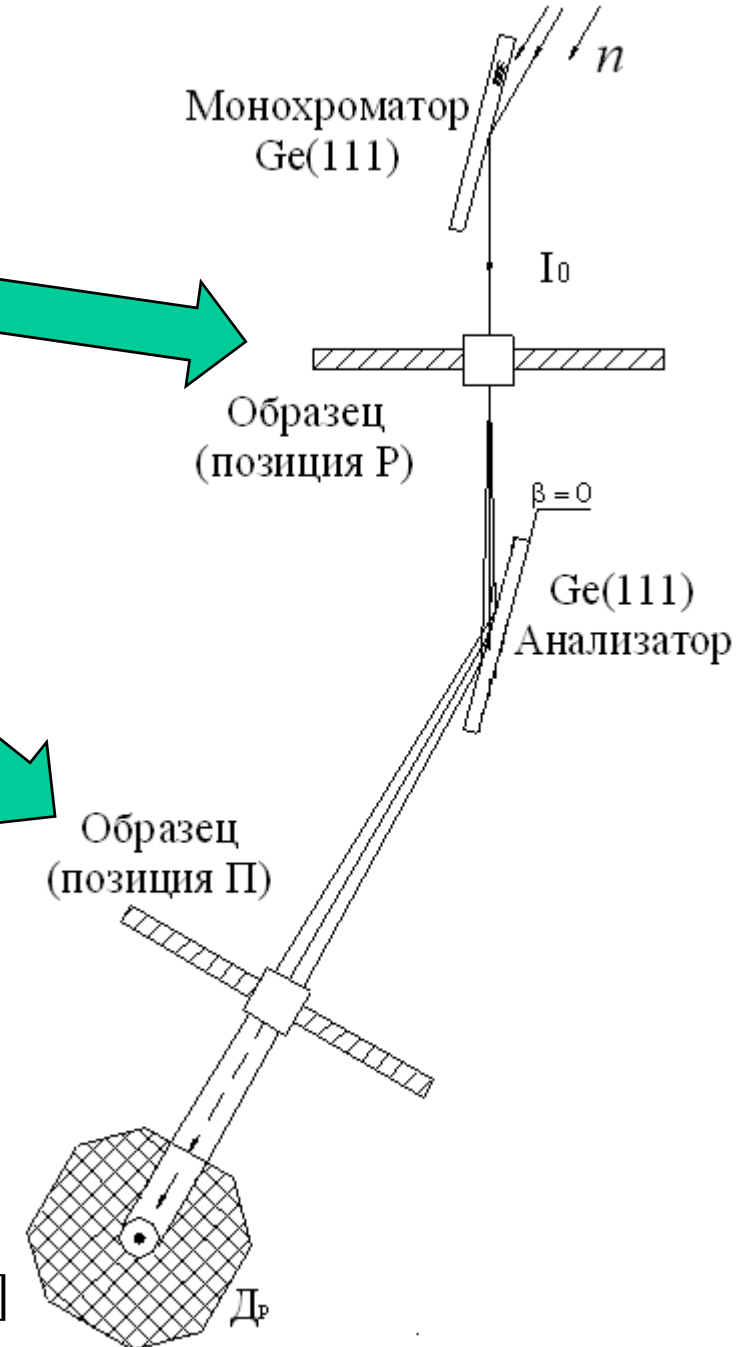
$$N/N' = T_S = \exp (-\Sigma_S \cdot L)$$

Σ_S [1/cm] – полное макроскопическое (интегральное) сечение МУР

$$\Sigma_S = \frac{1}{L} \cdot \ln \left(\frac{N'}{N} \right)$$

$$\Sigma_S = n \cdot \sigma_t$$

$$\sigma_t = 2\pi r^2 \cdot [1 - (2\sin\rho/\rho) + (2/\rho^2) \cdot (1 - \cos\rho)]$$



Метод Уоррена без перемещения образца

С образцом

$$N' = \varepsilon' \cdot T_0 \cdot T_{Ge} \cdot J_0$$

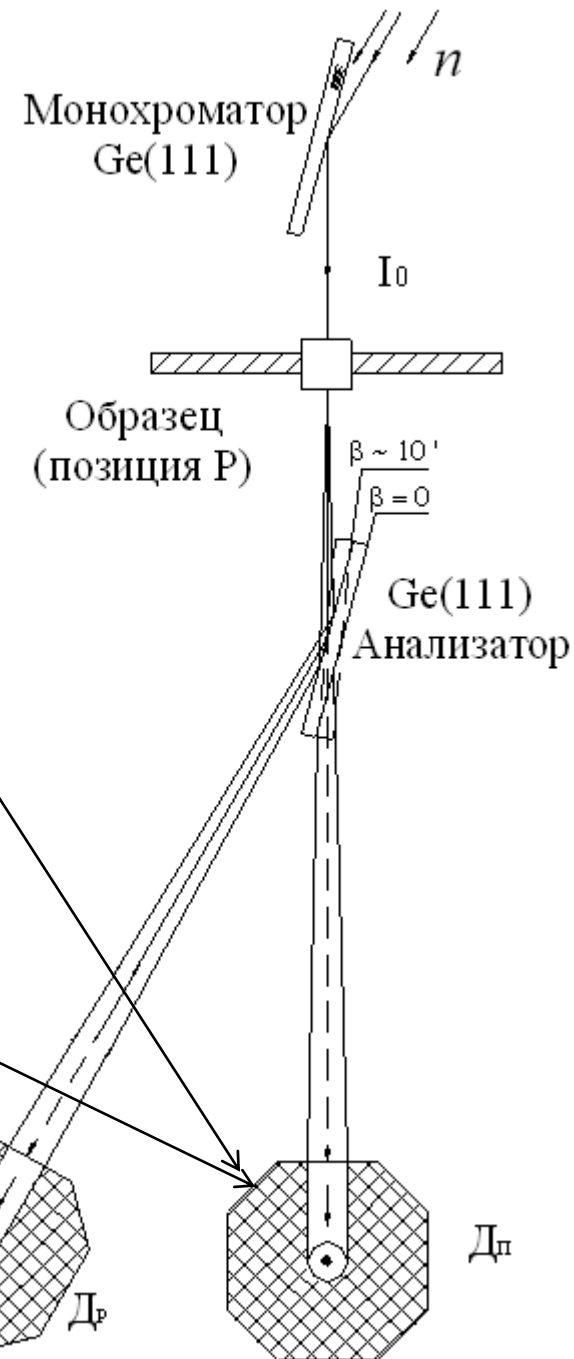
Без образца

$$N'_0 = \varepsilon' \cdot T_{Ge} \cdot J_0$$

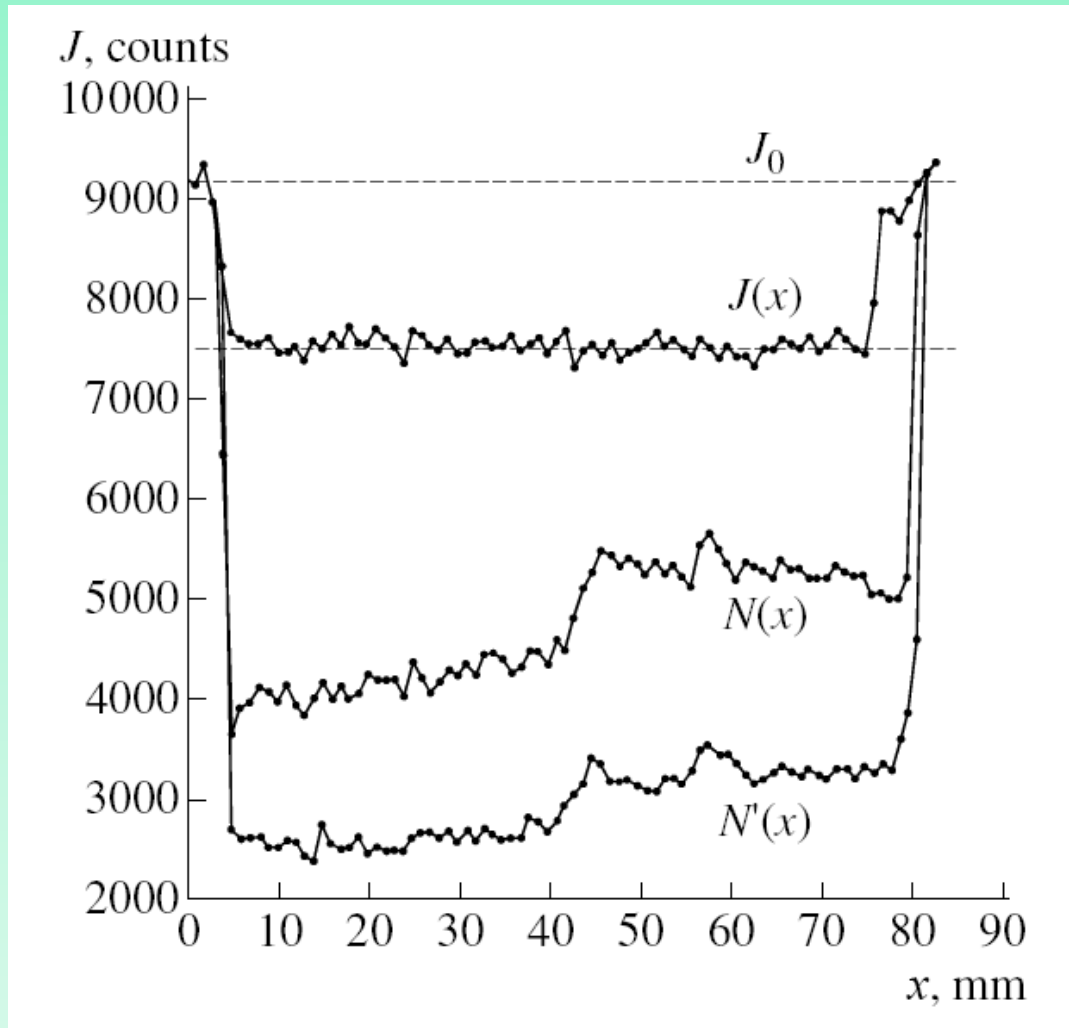
$$N_0 = I_{ins}(\beta = 0)$$

$$N = T_0 \cdot T_S \cdot I_{ins}(\beta = 0)$$

$$\Sigma_s = \frac{1}{L} \ln \left(\frac{N_0 \cdot N'}{N \cdot N'_0} \right)$$



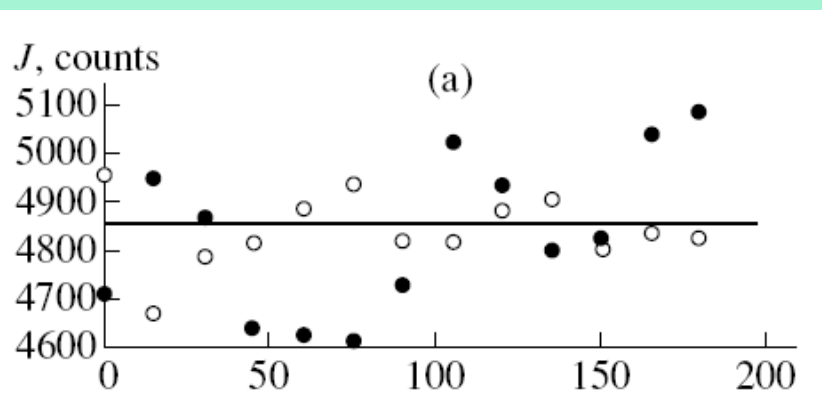
Results. Translational motion of the sample.



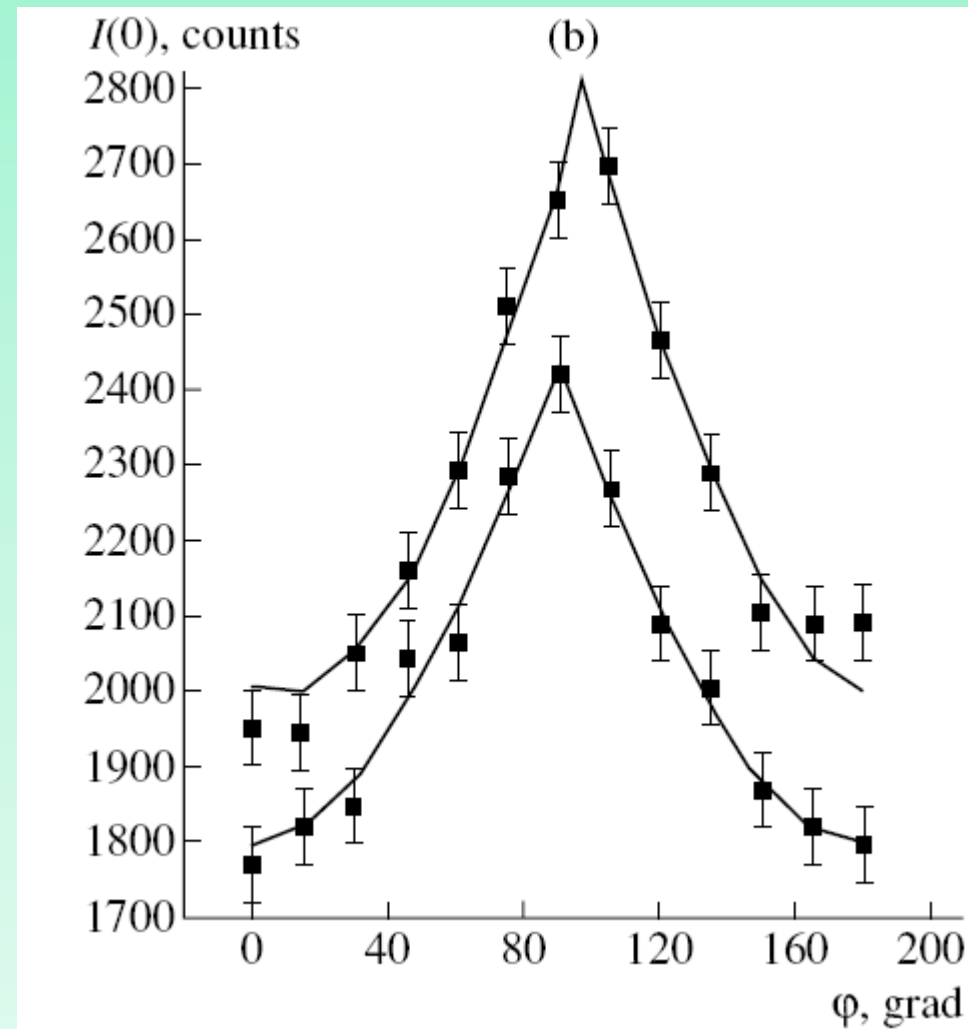
Neutron intensities vs. the coordinate x of the translational motion of the sample.

Results. Rotation of the sample.

$$I(0) = T_0 I_0 \left\{ 1 - c \sigma_t L \frac{|\cos \varphi|}{2 a k_0 \omega_0} \left(1 - \exp \left(-2 a k_0 \omega_0 / |\cos(\varphi - \varphi_0)| \right) \right) \right\}$$



Intensities of neutrons (a) passed through, J , and (b) reflected from, $I(0)$, the crystal analyzer vs. the angle of rotation about the horizontal axis. The upper and lower curves in Fig. 3b correspond to the lower (4.15 mm/h) and higher (10.9 mm/h) pulling rates, respectively.



Calculation of the intensity $I(0)$

In the case of a thin sample from the Molieres theory we obtain

$$I(0) = T_0(1 - c\sigma_t L)I_{ins}(0) + T_0 c L \int I_{ins}(\alpha_x) I(\alpha_x) d\alpha_x$$

$$I(\alpha_x) = \int_{-\infty}^{\infty} \sigma(\alpha_x, \alpha_z) d\alpha_z$$

The instrumental line $I_{ins}(\alpha)$ can be approximated by the Lorentz function

$$I_{ins}(\alpha_x) = \frac{I_0 \omega_0^2}{\alpha_x^2 + \omega_0^2}$$

Calculation of the differential scattering cross section

The neutron optical potential of vertical filament of a transverse size a

$$U = U_0 \theta(|x| < a) \theta(|y| < a)$$

The scattering amplitude is a Fourier transform of the potential

$$f(\mathbf{q}) = -\frac{4mU_0}{\hbar^2 k_0} \delta\left(\frac{q_z}{k_0}\right) \frac{\sin(aq_x)}{q_x} \frac{\sin(aq_y)}{q_y}$$

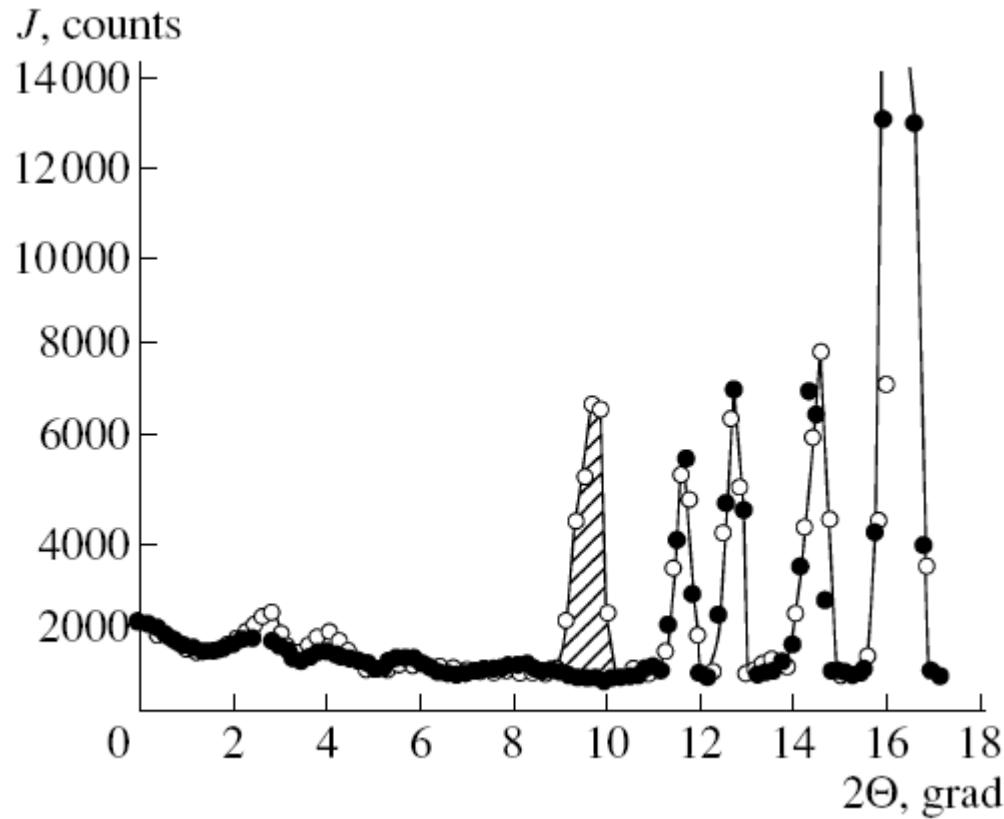
The differential cross section

$$\sigma(\mathbf{q}) = |f(\mathbf{q})|^2 = \frac{16m^2 U_0^2 a^2}{\hbar^4 k_0^2} \frac{\sin^2(aq_x)}{q_x^2} \delta^2\left(\frac{q_z}{k_0}\right)$$

The filament makes an angle ϕ with the vertical

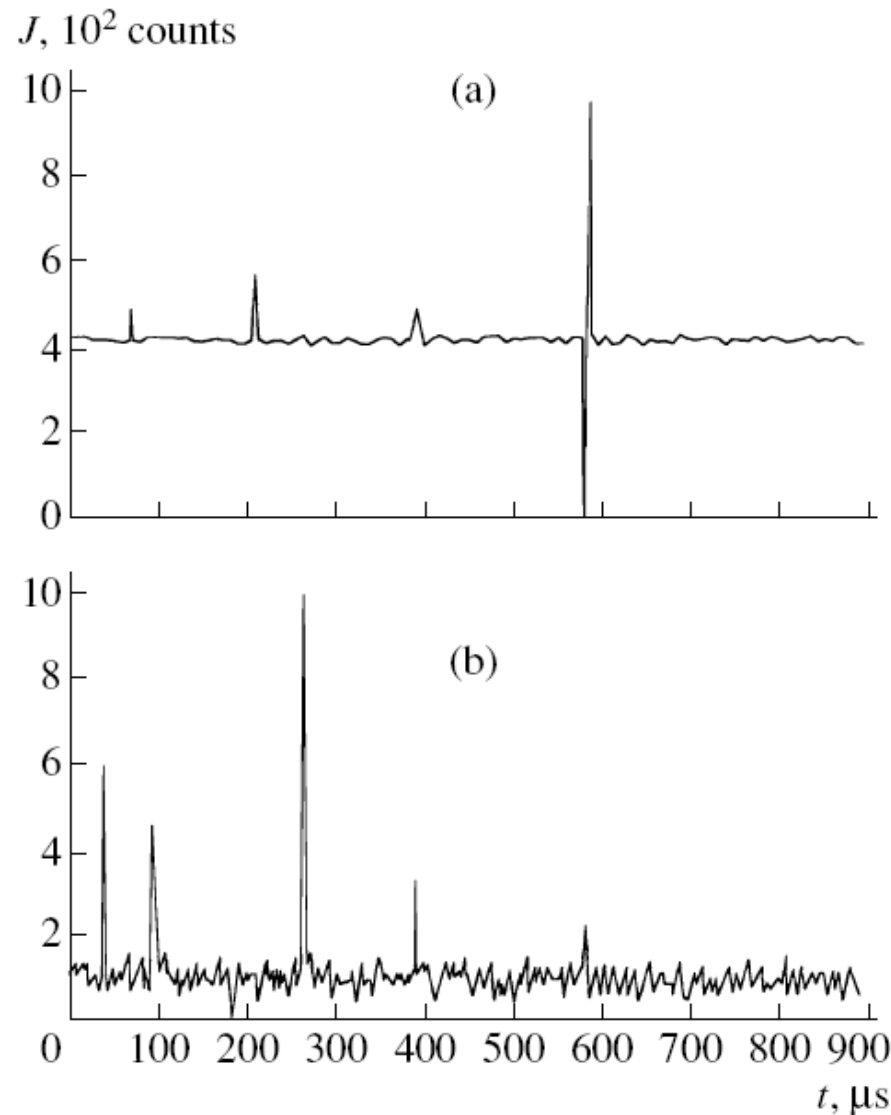
$$\sigma(\mathbf{q}) = A \frac{\sin^2(aq_x \cos \phi - aq_z \sin \phi)}{(q_x \cos \phi - q_z \sin \phi)^2} \delta^2(\alpha_x \sin \phi + \alpha_z \cos \phi)$$

Fragments of the neutron diffraction patterns taken at the constant wavelength $\lambda = 1.03 \text{ \AA}$ from two halves of the sample, which were grown at pulling rates $v1 = 4.15 \text{ mm/h}$ and $v2 = 10.9 \text{ mm/h}$.



All the diffraction reflections present on the pattern corresponding to the lower pulling rate are seen on the pattern corresponding to the higher pulling rate. However, the latter have a number of extra peaks (one of which is hatched).

Fragment of the transit-time neutron diffraction patterns taken from two halves of time. the sample. Pulling rate is (a) $v_1 = 4.15$ mm/h and (b) $v_2 = 10.9$ mm/h. t is the transit time



Conclusion

The structure of directionally solidified Al_2O_3 - $\text{Y}_3\text{Al}_5\text{O}_{12}$ ceramics grown from the melt with different pulling rates is studied by neutron diffraction and SANS. It is confirmed that the material grown with a pulling rate of 4 mm/h or below, is single-crystal Al_2O_3 densely penetrated by YAG filaments.

For pulling rates ranging from 4.14 to 10.9 mm/h, the filamentary structure of the $\text{Y}_3\text{Al}_5\text{O}_{12}$ phase persists and the matrix phase decomposes into crystallites. It is found that the limiting pulling rate at which the matrix remains single-crystalline lies within the 4–10 mm/h interval.

A direct correlation between the defect concentration and pulling rate is demonstrated. It is established that an increase in the pulling rate raises the number of inhomogeneities (defects) at grain boundaries in the single-crystal phase. Even minor variations of the pulling rate due to the unstable operation of the pulling mechanism have a significant effect on the defect concentration in the material grown. A change in the pulling rate does not affect the preferred growth direction of the filaments. This direction is the same as the pulling direction within the experimental error.

Бета-ЯМР спектроскопия

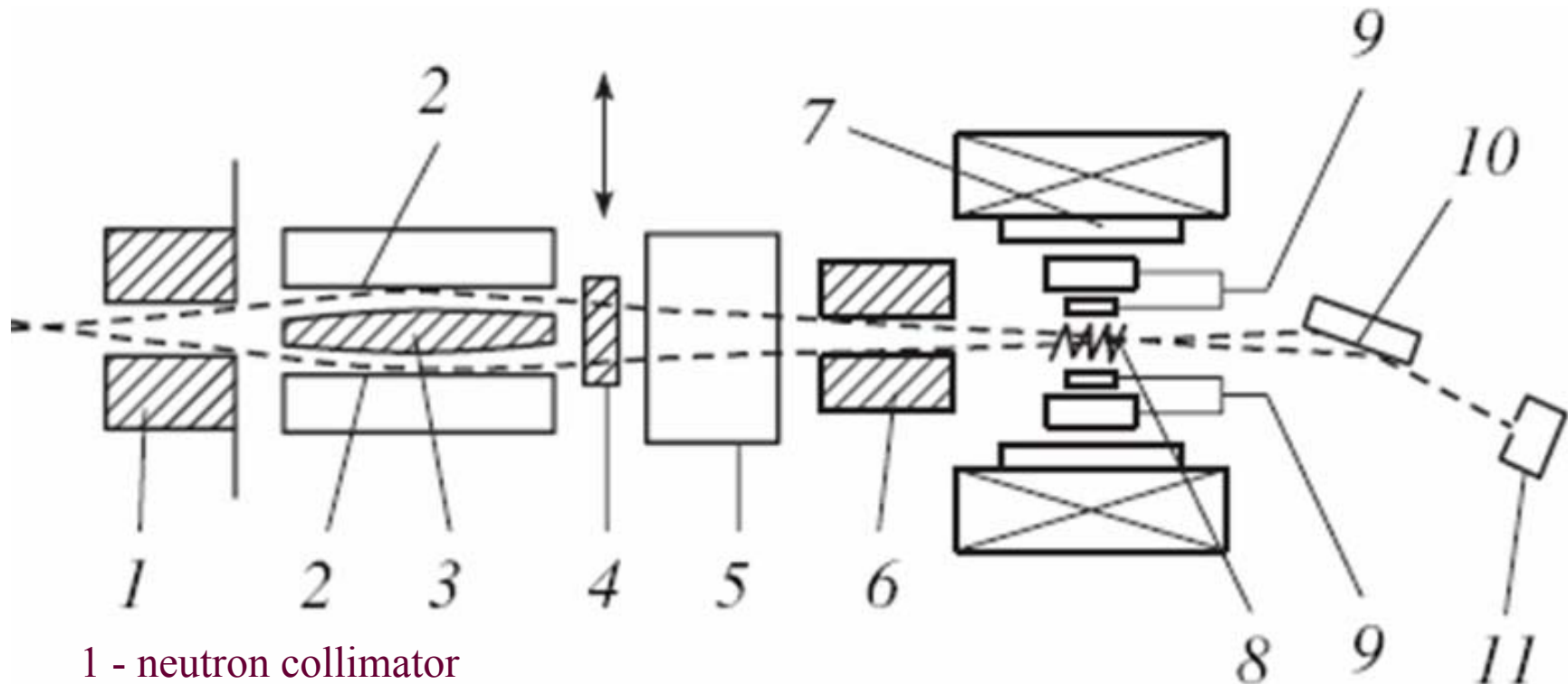
- β -ЯМР = магнитный резонанс и релаксация поляризованных бета-активных ядер
- β -ЯМР основан на наличии корреляции между ядерной поляризацией $P = \langle I \rangle$ и направлением k вылета электрона из β -активного ядра
 - $W(\vartheta) \sim 1 + a \cdot P(t) \cdot \cos \vartheta, \quad \cos \vartheta = kP/kP,$

Измеряется асимметрия

- $\varepsilon = (W(0) - W(\pi)) / (W(0) + W(\pi)) = a \cdot P(t),$

Здесь $a \sim 0.1$ — ядерная константа. Время $t = 0$ отвечает моменту создания β -активного ядра.

Схема β -ЯМР спектрометра



1 - neutron collimator

2 – polarizer of neutron beam, 3 - direct-beam absorber,

4 - chopper, 5 - spin-flipper, 6 - magnet-collimator,

7 - electromagnet, 8 - sample with rf-coil, 9 - β -counters,

10 - analyzer of neutron beam, 11 - neutron counter.

Процесс миграции поляризации по неупорядоченной системе ядер.

Рассматривается система ${}^8\text{Li}$ -
 ${}^6\text{Li}$. Главные особенности:

- 1) случайное распределение
 ${}^6\text{Li}$ в кристалле;
- 2) Уникальная близость g-
факторов

$$\frac{g({}^8\text{Li}) - g({}^6\text{Li})}{g({}^6\text{Li})} = 0.0057$$

Перенос поляризации описывается уравнением:

$$\frac{dp_{im}}{dt} = - \sum_j (\nu_{ji} p_{im} - \nu_{ij} p_{jm}), \quad p_{im}(t=0) = \delta_{im},$$

где i, j, m — номера занятых примесью узлов правильной решетки L ,

p_{im} — вероятность обнаружить поляризацию (возбуждение) в узле i в
момент времени t , если в начальный момент времени она была в узле m .

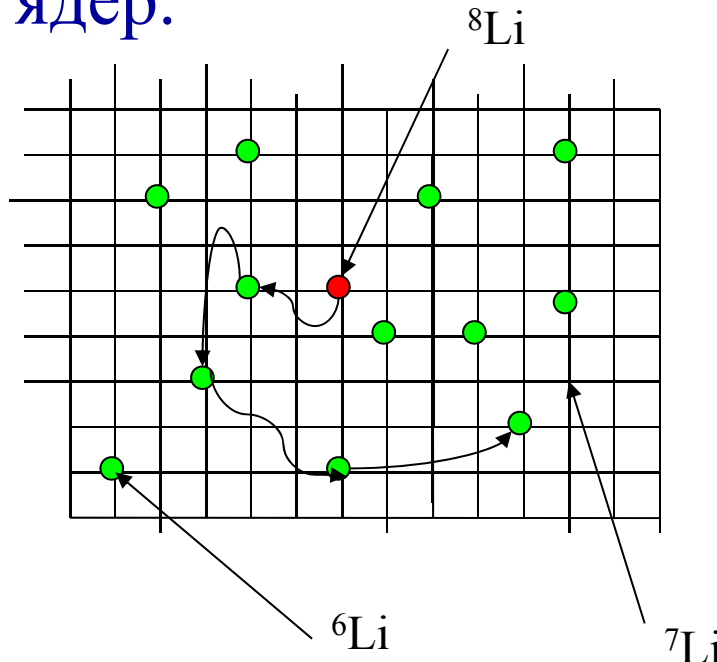
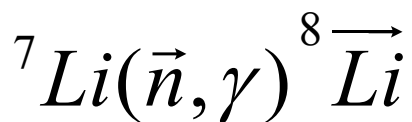
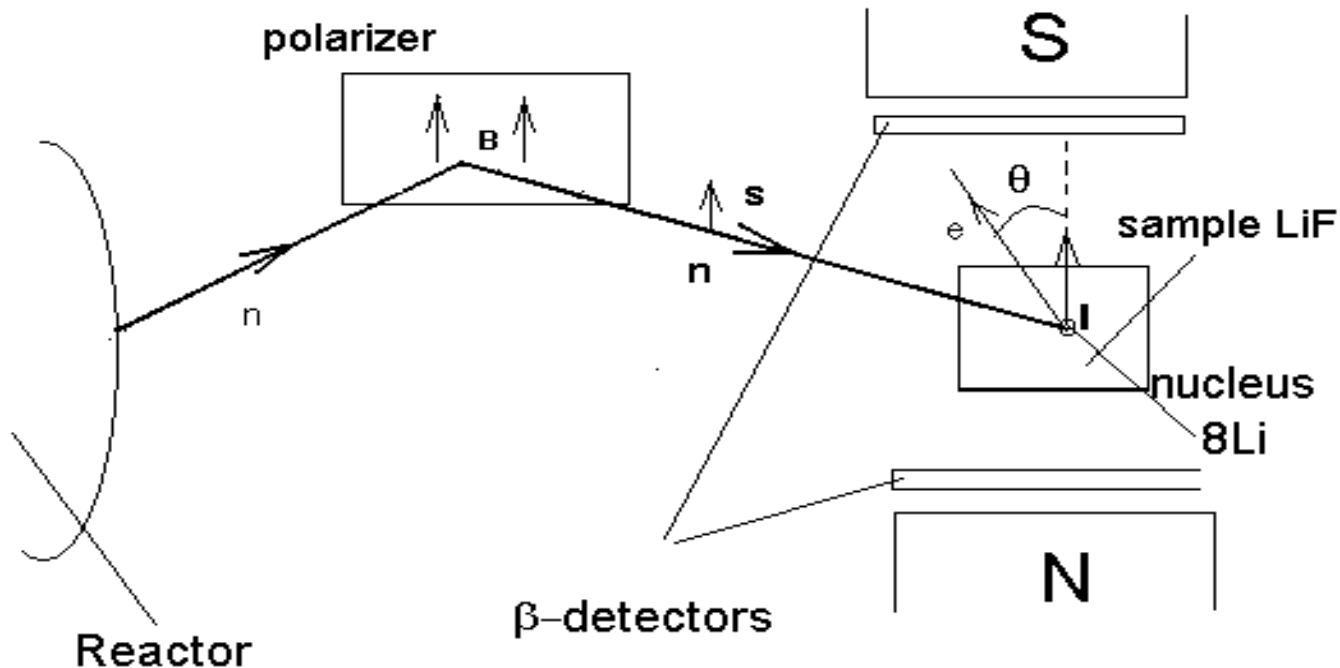


Схема процесса.

Схема эксперимента.

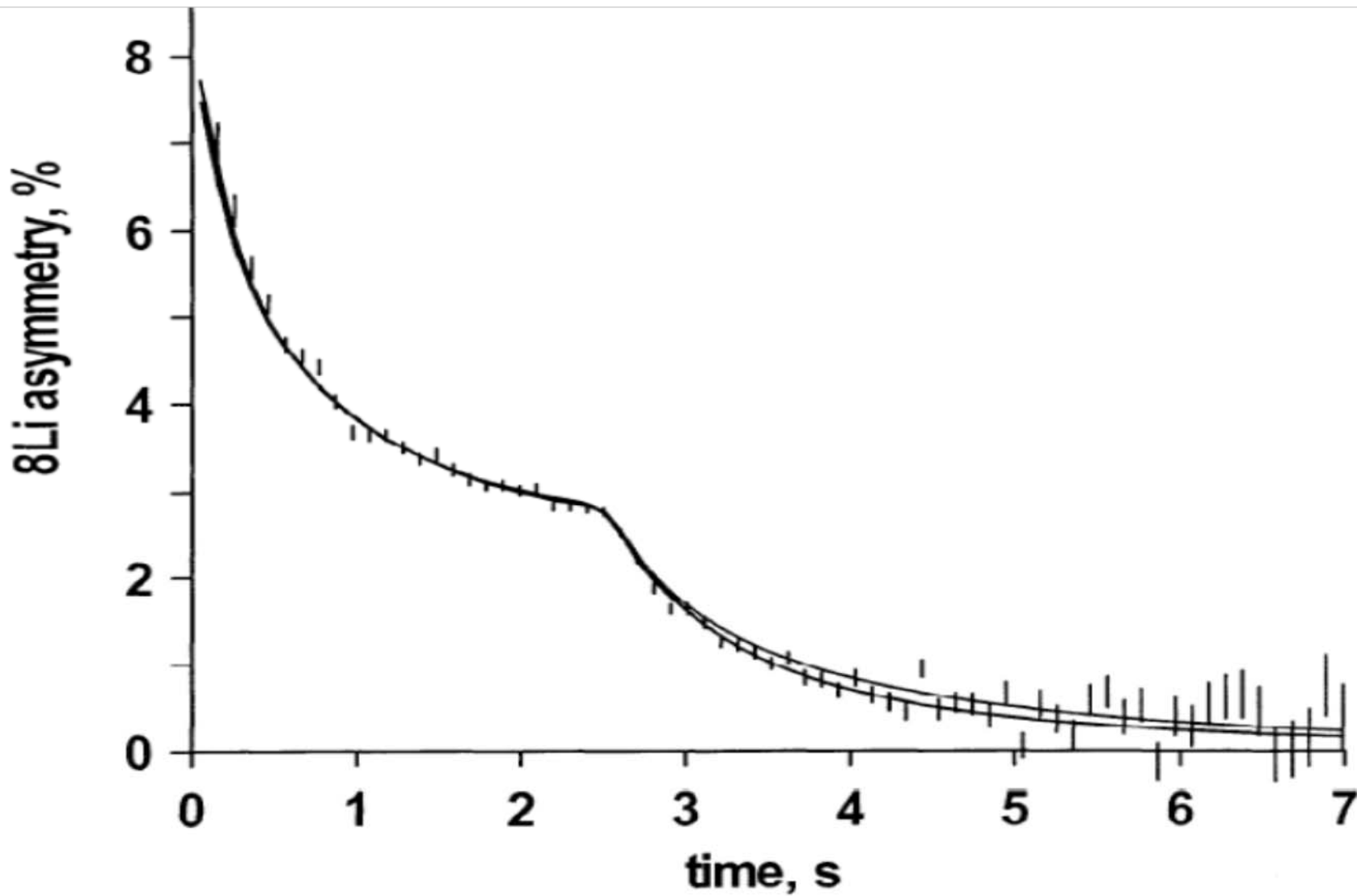


Угловое распределение β -излучения

$$W(\theta, t) \sim 1 + a \cdot p(t) \cdot \cos \theta$$

Измеряется величина

$$\varepsilon = \frac{N(\theta = 0, t) - N(\theta = \pi, t)}{N(\theta = 0, t) + N(\theta = \pi, t)} \Leftrightarrow a \cdot p(t)$$



Comparison of the theoretical line (upper curve) with experimental data and with formal fitting line (lower curve).

The Nobel Prize in Physics 1994



"for pioneering contributions to the development of neutron scattering techniques for studies of condensed matter"

Neutrons show
what atoms do

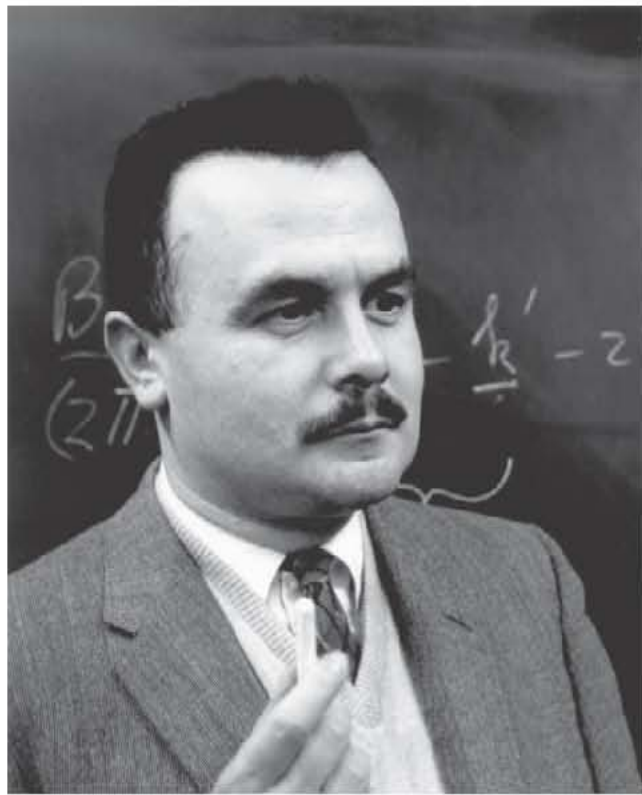


Bertram N. Brockhouse

"
n
e"



Clifford G. Shull



“If the neutron did not exist, it would need to be invented.”

- B. Brockhouse